GaSe$_{1-x}$S$_x$ second harmonic generators for CO$_2$ lidars

Y. Qu,[1] Z.-H. Kang,[1] T.-J. Wang,[1] Yu.M. Andreev,[2] G.V. Lanskii,[2] A.N. Morozov,[3] and S.Yu. Sarkisov[2]

[1]Jilin University, Changchun, China
[2]Institute of Monitoring of Climatic and Ecological Systems,
Siberian Branch of the Russian Academy of Sciences, Tomsk, Russia
[3]Siberian Physical Technical Institute, Tomsk, Russia

Phase matching conditions, damage threshold, nonlinear and thermal properties of solid solution crystals GaSe$_{1-x}$S$_x$ with the mixing ratio $x \leq 0.4$ have been studied. Tunable CO$_2$ laser SHG with GaSe$_{0.867}$S$_{0.33}$, GaSe$_{0.71}$S$_{0.29}$, and GaSe$_{0.6}$S$_{0.4}$ were investigated. The CO content in the atmosphere was measured with the lasers, being in the composition of TT differential absorption lidars.

Introduction

On-line monitoring of the atmospheric gas composition is the issue of the day because of the strong environmental worsening, which adversely impacts on people and nature. Optical measuring techniques and instrumentation, based on the use of laser radiation sources, are widely used for the problem solution. Owing to the largest interaction cross-section between optical radiation and atmospheric gases, as well as the instrumentation simplicity, the differential absorption technique has advantages over other optical methods, that is proved by practical results.

Real-time monitoring of trace gas concentrations is carried out in the real atmosphere using mainly differential lidars — gas analyzers of different types. Most of them are so-called path meters, measuring the path-averaged gas concentrations with the use of specular reflectors or topographical targets (TT) as reflectors (TT lidars) in the middle IR range. Intensive resolved spectral structures and isolated absorption lines of almost all atmospheric gases, suitable for measurements, are present in this range.[1,2]

The CO concentration is of great interest, because the gas is one of the most common and toxic atmospheric gases, the concentration of which permanently recovers due to vehicular, industrial, and natural emissions. To provide for a high path measurement accuracy (at a level of units and tens of ppb) when working on CO radiation baseband lines centered near 4.7 μm, the second harmonic generators (SHG) of the 9-μm band of low-pressure CO$_2$ lasers have shown themselves in a good light.

These effective, reliable, and available lasers have narrow laser bands (about $2 \cdot 10^{-3}$ cm^{-1}) far-distant from each other (1.5—2.0 cm^{-1}) with certainly known spectral positions. Such spectral parameters of laser bands allow one to avoid the use of complex optical systems for their formation, at least when measuring in the ground atmosphere, and to provide for computer-controlled choice of required laser lines using simple mechanical step motors.[3–5] Energy parameters of the frequency doubled radiation of pulsed-periodic low-pressure CO$_2$ lasers are sufficient to determine the above-background CO concentrations, particularly, when working with 100-m distant topographic objects.[5]

However, high performance characteristics of CO$_2$ lasers and a high potential of the differential absorption technique, supported by virtually perfect matching of SHG lines and the absorption line intensities,[5] are incommensurate to the popularity of CO$_2$ lidars with frequency doublers in monitoring the CO atmospheric concentration.

Disadvantages in performance of nonlinear crystals used as SHG cause such state of things. CdGeAs$_2$ crystals operate only at cryogenic temperatures in order to decrease the absorption by free charge carriers to some acceptable level.[3] ZnGeP$_2$ crystals require a wide range ($\pm 45°$) angular tuning to the synchronism direction throughout generation range, which in turn requires permanent adjustment of the lidars' optical tract while measuring. In this case, frequency doubling of 10-μm band CO$_2$ lines, necessary for a permanent expansion of the number of gases under control, is possible in them only at heating up to 200—300°C [Ref. 6].

CdGeAs$_2$ crystals are characterized by a high, about 1 cm^{-1} and more, optical loss at the second harmonic wavelengths, while ZnGeP$_2$ — by the same level of loss at the wavelengths of CO$_2$ laser baseband, limiting the efficiency of the frequency conversion. Both crystals are non-transparent at wavelengths of visible lasers, which does not allow their use for initial tuning of lidar optical tracts and retuning while measuring. Other types of nonlinear crystals have low performance characteristics and are unusable in TT lidars in the routine mode.[6]

In this work, different nonlinear crystals are compared and evaluated as CO$_2$ laser SGH in differential absorption TT lidars, among them the widely used GaSe and AgGaS$_2$ crystals, little used and new LiInSe$_2$ and HgGa$_2$S$_4$ crystals, solid solution

crystals $AgGaGe_xS_{2(1+x)}$ with $x = 1$; $Hg_{1-x}Cd_xGa_2S_4$, $x = 0.11$; and $GaSe_{1-x}S_x$, $x = 0.133$, 0.29, and 0.4. The CO concentration in the atmosphere was *in-situ* measured using $GaSe_{1-x}S_x$-based SHG.

1. Experimental study of SHG

Two grating-tunable low-pressure CO_2 lasers of our making were used as pumping sources for nonlinear crystals. Their parameters were optimized for path measurements with the use of specular reflectors and topographic targets as the reflectors, respectively.

The first laser operates on the mixture $Xe:CO_2:N_2:He = 1:2.5:2.5:17.5$ with a total pressure of 20 Torr in the pulse-periodic mode at the pulse frequency up to 600 Hz. A highly-stabilized shutter with modulation rate variations ≤ 0.5 Hz, mounted in the focus of intracavity lens system, allows radiation pulses with the length of leading peaks of about ~120 ns and a peak power of $0.1-1$ kW at different lasing lines. In this case, about a half of total pulse energy contains in the nitrogen "tail" of $5-6$ μs pulse.[7]

The second laser, having the passive mechanical, temperature, magnetostriction, and piezoelectric cavity length stabilization, operates on the mixture $CO_2:N_2:He = 1:1:6$ at a working pressure of 15 Torr and a mean output power of up to 5 W in the TEM_{00} mode. The same shutter allows a highly carrier-stabilized quasi-sinusoidal radiation to be obtained and the Unipan 237 selective nanovoltmeters (Poland) for precision measurements of electric signals to be used.[8]

CO_2 lasing lines are chosen by the computer-controlled positioning device RCA100, Zolix Instruments Co., Ltd, China, with an angular positioning error of $\pm 4.5''$, allowing tuning to required lasing lines and maximizing laser output energy parameters.

The SHG is assembled following a standard optical circuit. Nonlinear crystal is adjusted to the synchronism direction with a RCA100 positioning device, which allows a decrease of the total synchronism angle error down to an acceptable level of $\pm 10'$.

To determine the SHG spectral parameters and to conduct lidar measurements, the lasing lines were chosen with the use of 66 gr./mm-grating computer-controlled monochromator SBP300, Zolix Instruments Co., Ltd, Chine. The ZnSe lens with a 100-mm focal length was used for focusing the pumping beams into crystals, mounted in the oven with a controllable temperature between the room one and 300°C at about ~1°C accuracy. The oven was used to determine the temperature dispersion of the synchronism conditions.

Radiation pulses were recorded with the liquid nitrogen MCD-photoresistor with the 0.5×0.5 mm sensitivity area and a time constant of about ~8 ns, as well as with a pyroelectric detector PCI-L-3, Vigo System S. A. (Poland) with the following

characteristics: a spectral sensitivity range of $2-12$ μm, a sensitivity area of 1×1 mm, and a time constant of < 1 ns. Temporal behavior of the recorded pulses was analyzed with a two-channel oscillograph TDS3052, Tektronix Inc., with the 500 MHz passband and 1.3-ns time constant. Pulse energy was measured with a calibrated pyroelectric detector.

As SHG, we used millimeter-size elements, made of GaSe, $LiInSe_2$, $HgGa_2S_4$, and $AgGaS_2$ crystals and solid solution of nonlinear crystals $AgGaGeS_4$ (obtained as $AgGaS_2:GeS_2 \rightarrow AgGaGe_xS_{2(1+x)}$, $x = 1$), $Hg_{0.79}Cd_{0.11}Ga_2S_4$ ($HgGa_2S_4:CdGa_2S_4 \rightarrow Hg_{1-x}Cd_xGa_2S_4$, $x = 0.11$), $GaSe_{0.867}S_{0.133}$, $GaSe_{0.71}S_{0.29}$, and $GaSe_{0.6}S_{0.4}$ ($GaSe:GaS \rightarrow GaSe_{1-x}S_x$, $x = 0.133$, 0.29, and 0.4).

Approximately, 1-% decrease of S concentration relative to the growth stimulant composition and the same level of variations of its concentration in the crystal volume has been noted in the chemical composition of the grown and used solid solution crystals $GaSe_{1-x}S_x$, $x = 0.133-0.4$ was determined by the electron emission spectroscopy method, using the emission microscope JEO 1430 (Japan). At $x \leq 0.4$, crystals keep noncentrosymmetric point symmetry group $\bar{6}2m$ and ε-structure (determined by the Transparency Electron Microscopy (TEM) and Reflection High Energy Electron Diffraction (RHEED) methods), transforming into unsuitable centrosymmetric or hybrid structures at $x > 0.4$. The shortwave transparency spectrum boundary of $GaSe_{1-x}S_x$ crystals displaces from 0.62 μm at $x = 0$ to 0.52 μm at x rising to 0.4. The set of nanohardness versus indentor weight and doping level curves, as well as mixing ratios justified that the nanohardness rise stops at $x > 0.4$ and the mixed crystal structure changes.

Samples of all crystals were made with the orientation to SHG of CO_2 laser 9-μm band by the first type of three-frequency interactions, except for lamellar crystals GaSe and $GaSe_{1-x}S_x$, made by the cleavage method. Their optical axes are normal to the growth layers. All crystals are characterized by the optical loss coefficients $\alpha \leq 0.05$ cm^{-1} within the maximal transparency region, which has been calorimetrically measured from the time of reaching the stable temperature of vacuumed crystals under the action of continuous CO laser radiation of quite high (watt level) power. Using a Shimazdu UV 3101PC spectrophotometer (operating range of $0.3-3.2$ μm), it has been also ascertained that the studied crystal transparency spectrum begins from $0.35-0.62$ μm wavelengths by the 10-% level.

The influence of optical loss on SHG efficiency is negligible in samples of the $2-3$ mm (in length) nonlinear crystals of such optical quality. They allow the use of He–Ne 0.63-μm radiation and diode lasers of 0.7-μm radiation for tuning the lidar optical tract. The only exception is the $LiInSe_2$ crystal, which would not do in CO_2 lidars, because it is characterized by a significant coefficient of optical loss (0.5 ± 0.05) cm^{-1} at wavelengths of CO_2 laser 9-μm band, negating the efficiency of the second harmonic generation, and non-transparency at wavelengths of 10-μm band.

It is known that the efficiency of parametric frequency conversion in optically qualitative nonlinear crystals with an appropriate transmittance spectrum is determined, first of all, by nonlinear optical and thermal characteristics and the damage threshold. Study of the damage threshold of $Hg_{0.89}Cd_{0.11}Ga_2S_4$, $HgGa_2S_4$, $AgGaGeS_4$, $AgGaS_2$, $LiInSe_2$, and GaSe crystals by the technique described in Ref. 8, has shown the 1:1.1:0.83:0.84:0.88:0.43 ratio of its values for 9.6 μm wavelength. In this case, the quality factors ratio is $M = d^2/n^3 = 1:0.97:0.06:0.08:0.11:1.28$, where d is the second order nonlinear susceptibility coefficient; n is the average refractive index of the crystal at wavelengths of the interacting radiations.

When calculating the quality factor, the nonlinear susceptibility coefficient of the second order was taken equal to the commonly used values from Ref. 10, while $M = 111$ pm/V for the solid solution crystal $Hg_{0.89}Cd_{0.11}Ga_2S_4$ was calculated by the weighted-average-square method using data on the initial crystals.[11] For GaSe crystals, having large spread in values of the nonlinear susceptibility coefficient,[10] $d_{22} = 54$ mp/V was accepted.

It may be supposed that the solid solution crystals $Hg_{1-x}Cd_xGa_2S_4$ are the most promising for further development of the growing technique. When changing mercury atoms for lighter cadmium ones, the thermal conductivity and, hence, the damage threshold are to increase at almost similar nonlinear properties of initial $HgGa_2S_4$ and $CdGa_2S_4$ crystals.[11]

Optical breakdowns in new GaSe samples were most often observed in the crystal volumes, but not on their entrance surfaces. The damage threshold was by 1.3–3-times lower than the surface one. The internal breakdowns in the grown $GaSe_{1-x}S_x$ crystals disappeared probably due to disappearance of microcavities in their layered structure. The damage threshold of non-polished surfaces of $GaSe_{1-x}S_x$ crystals ($x \geq 0.133$; made by cleavage technique) was about two-time higher as compared to those of pure GaSe crystals and close to those of $ZnGeP_2$ crystals, which are so-called "middle IR nonlinear crystal standard."[12] The damage threshold did not increase with x rise.

Note that the efficiency of frequency conversion is proportional to M [Ref. 10], while the limiting efficiency — to the product of damage threshold and quality factor under the supposition of similarity of thermal properties of the considered crystals. The following crystal order by their catching to use in TT lidars is evident from the quality factor calculations, accounting for the obtained data on the damage threshold and large optical loss in $LiInSe_2$ crystals:

$$HgGa_2S_4 : Hg_{0.89}Cd_{0.11}Ga_2S_4 : GaSe_{1-x}S : AgGaS_2 =$$
$$= 1.07 : 1 : 0.55 : 0.03.$$

These are uniaxial crystals. $AgGaS_2$ crystals are evidently unpromising for lidar applications.

One more important parameter of nonlinear crystals is the thermal conductivity, determining the limiting efficiency of frequency conversion and crystal place in applied devices. The lower is the thermal conductivity, the smaller is pumping intensity values, at which thermal lens is formed into a crystal, which results in the surface fracture. Table presents the thermal conductivity, measured in parallel ($\|C$) and perpendicular ($\perp C$) to the optical axis with an IT-λ-400 meter by a thoroughly worked out technique with an error not exceeding ±15%.[13]

It is evident, that GaSe and $GaSe_{1-x}S_x$ crystals have a maximally high thermal conductivity among the studied ones (by 5–10 times), which is about two times exceeded only by $ZnGeP_2$ crystals (0.365 W/(cm · K)).[10] Noticeable changes in the thermal conductivity along the $GaSe_{1-x}S_x$ crystal growth layers with x rise up to 0.4 have not been noted, while orthogonal to them it increases by a factor of four.

These features of thermal conductivity variations can explain the above-noted $GaSe_{1-x}S_x$ crystal damage threshold level keeping at the varying x. At a constant thermal conductivity along the growth layers and in the presence of small gradient of the pumping beam intensity orthogonal to the growth layers in optically qualitative crystals (and, consequently, small temperature gradient along the beam direction), the thermal conductivity and heat diffusion in the growth layer plane towards the periphery crystal side are the only important parameters. It also follows from the data on thermal conductivity, that biaxial nonlinear $LiInSe_2$ and $AgGaGeS_4$ crystals are not of interest to TT lidars because of their potential and, especially, limiting SHG efficiency.

Thus, taking into account the improved damage threshold of solid solution $GaSe_{1-x}S_x$ crystals in comparison with pure GaSe, the keeping and even some increase of the thermal conductivity, a lower level of optical loss (0.1 cm^{-1} against 0.57–1.0 cm^{-1}), and about 10-% lower refractive index value at CO_2 laser wavelengths in comparison with $ZnGeP_2$ allows these crystals to lead among the most promising middle-IR nonlinear crystals. Once nonlinear properties and phase synchronism conditions, determining the values of their effective nonlinear susceptibility have been studied, the final conclusion about the crystals' place can be drawn.

Table. Thermal conductivity of nonlinear crystals

Crystal		$Cd_{0.11}Hg_{0.89}Ga_2S_4$	$HgGa_2S_4$	GaSe	$GaSe_{1-x}S_x$	$AgGaS_2$	$AgGaGeS_4$	$LiInSe_2$
Thermal conductivity, W/(cm·K)	$\|C$	0.057 ± 0.009	0.039 ± 0.004	0.162	0.162 ± 0.1	0.009 ± 0.001	0.014 ± 0.002	0.014
	$\perp C$			0.020	0.086 ± 0.03			0.015

Note, that improvement of nonlinear optical properties of GaSe crystals by sulfur and indium doping allowed about 80-% increase of the second harmonic generation efficiency in the doped crystals in comparison with pure GaSe ones.[4,5] In this case, a 8-fold increase of hardness and layer cleavage decrease made the growth layer cleavage difficult to be realized and allowed performance characteristics of working elements under field conditions to be enhanced. This also allowed their mechanical treatment, including polishing. Thus, production of crystal samples of any orientation became possible.

Comparison of experimentally measured rate of synchronism angle variations at CO_2 laser SHG in $GaSe_{1-x}S_x$ crystals with x rise has shown it to be almost 3-fold slower than in model estimations with the use of data on dispersion properties of $GaSe$[9] and GaS[14] crystals. However, the correspondence between experimental results and estimations is quite good for pure crystals, which is the evidence of the correctness of data on dispersion properties of GaSe crystals and their incorrectness for GaS ones.

The comparison of CO_2 laser 9-μm band SGH efficiency with the model estimation of nonlinear coefficients by the technique from Ref. 15 has shown that a good agreement is obtained under the assumption that with x rise the second order nonlinear susceptibility coefficient takes its real value of about 70–75 pm/V, not screened by the cleavage defect. Then about 40-% decrease of nonlinear susceptibility coefficient, caused by the replacement of 40% of selenium atoms to sulfur ones ($x = 0.4$), is virtually compensated by the 30–40-% increase of the GaSe second order nonlinear susceptibility coefficient.

It may be supposed that qualitative polishing of $GaSe_{1-x}S_x$ crystals can result in essential increase of the damage threshold and in addition rise in SHG efficiency, always observed for other crystals. If the mechanical properties of $GaSe_{1-x}S_x$ crystals are appropriate for field conditions and their transparency spectrum is virtually the same as of the competing $HgGa_2S_4$ and $Hg_{1-x}Cd_xGa_2S_4$ spectra,[16] the former have great advantages over the latter ones: the simplicity of the growing technique, large yield, smaller (by several times) price. They allow the use of visible range lasers in tuning optical tracts of frequency converters, based on these crystals, and applied optical devices.

2. Application of the crystals to TT lidars

The CO_2 laser SHG of the 1st and 2nd types were under evaluation in composition of the TT differential absorption lidars when monitoring the carbon oxide in the atmosphere. An active model of TT lidar was first tested in the laboratory conditions (Fig. 1a), where it showed its efficiency in cell measurements[17] with the use of the pulse-periodic laser with intracavity radiation modulation.[7] Then it

was mounted in a mobile van, where the extracavity quasi-sinusoidal modulation laser was used.

Daily variations of CO concentration in urban atmosphere were measured with CO_2 laser quasicontinuous Q-spoiler at 1-m measuring path and a specular reflector in the total sensing beam interception mode by the technique from Ref. 6. The whole optical tract was tuned with a He–Ne laser of 1 mW in power.

Real-time measurement results are shown in Fig. 1b. The measurement error was determined with a brought calibration cell with a known amount of detectable gas and did not exceed ± 4 ppb·km in first experiments. Working samples of solid solution $GaSe_{0.867}S_{0.133}$, $GaSe_{0.71}S_{0.29}$, and $GaSe_{0.6}S_{0.4}$ crystals did not show any signs of failure after numerous lidar transportation and weekly field testing cycles interrupted only by the instrument adjustment.

Conclusion

Physical properties of solid solution nonlinear crystals, obtained by the scheme $GaSe:GaS \rightarrow GaSe_{1-x}S_x$, $0.133 \le x \le 0.4$, determining the parametric frequency conversion efficiency have been studied for the first time, as well as the performance characteristics of the SHG based on these crystals. The SHG have been tested within mobile path atmospheric CO meters.

A 8-fold increase of $GaSe_{1-x}S_x$ crystal nano-hardness with the increase of x up to 0.4, displacement of short-wave absorption edge from 0.62 to 0.52 μm, the increase of the nonlinear susceptibility coefficient up to 70–75 pm/V and the damage threshold up to that of $ZnGeP_2$ crystals, as well as a 4-fold increase of the thermal conductivity normal to the growth layers provide for keeping the efficiency of CO_2 laser second harmonic generation in $GaSe_{1-x}S_x$ ($0.133 \le x \le 0.4$) in comparison with pure lamellar GaSe crystals at increasing x, as well as essential superiority of the performance characteristics. Mechanical treatment, polishing, and, consequently, production of samples of a required orientation and the use of them within mobile lidar systems became possible.

The competition potentiality of the crystals by the second harmonic generation has been ascertained in comparison with other well-known middle-IR crystals: $AgGaS_2$, $AgGaGeS_4$, $LiInSe_2$, $HgGa_2S_4$, and $Hg_{1-x}Cd_xGa_2S_4$. Advantages of these crystals over $ZnGeP_2$ ones are: the possibility to use the visible spectrum lasers for tuning both SHG and the entire optical path during lidar operating, as well as a low price and the availability. This makes actual the addition researches of redefining phase matching conditions as the function of mixing ratio, the dependence of the damage threshold on the quality of working surface polishing; as well as comparative study of the second harmonic generation efficiency in similar experimental conditions relative to commonly used nonlinear crystals and of long-term performance characteristics of the solid solution crystals.
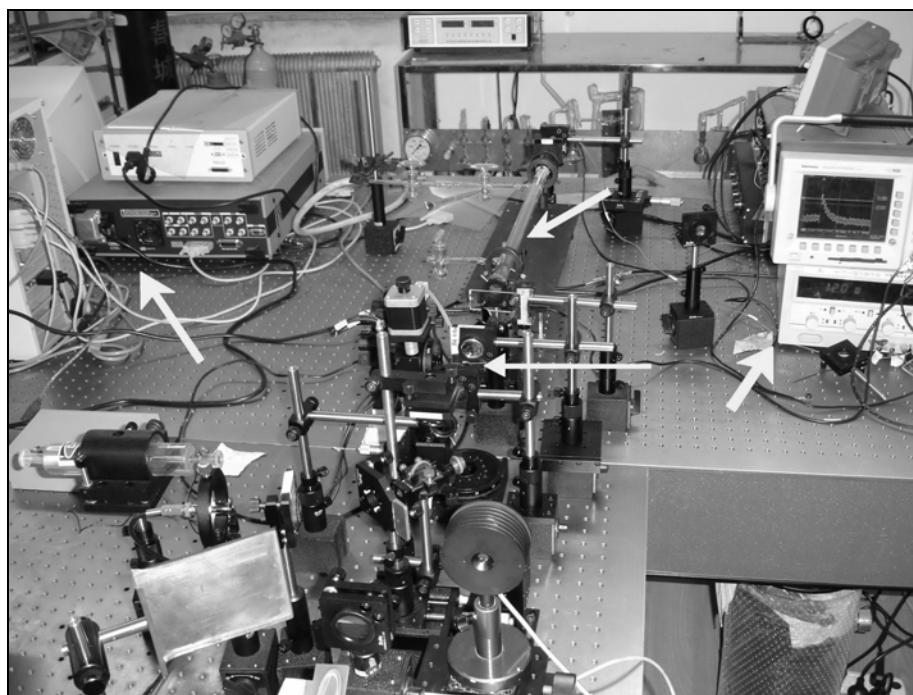
a
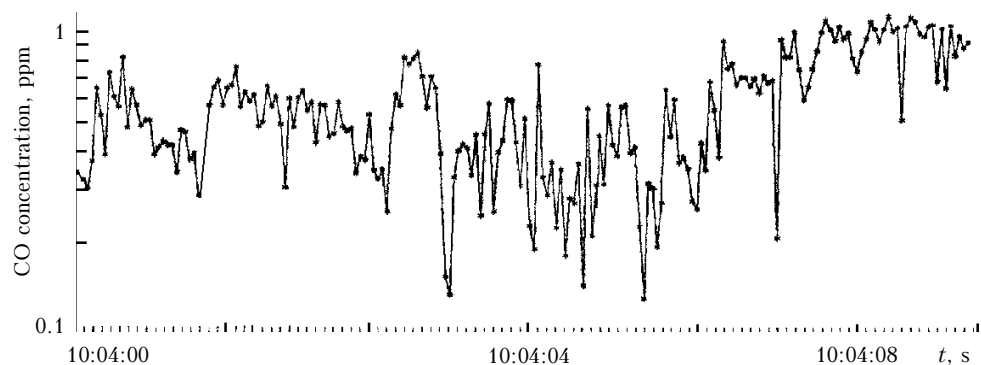
b

Fig. 1. Active model of TT lidar. Arrows point to the SHG unit at the center, the gas-filled cell is at top-center, digital and electronic monochromators are at the top-left and top-right, respectively (*a*); results of short-term *in-situ* CO measurements in the atmosphere (*b*).

References

1. E.D. Hinkley, ed., *Laser Monitoring of the Atmosphere. Topics in Applied Physics* (Springer-Verlag, New York, Heidelberg, 1976), V. 14, 380 pp.

2. R.M. Measures, ed., *Laser Remote Gas Analysis* (Jon Wiley & Sons, New York−Chischester−Brisbane−Toronto−Singapore, 1988), 546 pp.
3. D.K. Killinger, N. Menyuk, and W.E. DeFeo, Appl. Phys. Lett. **36**, No. 6, 402−405 (1980).
4. Yu.M. Andreev, V.E. Zuev, M.V. Kabanov, V.G. Voevodin, P.P. Geiko, A.I. Grebenyukov, and V.V. Zuev, Izv. Akad. Nauk SSSR, Ser. Fiz. **52**, No. 6, 1142−1149 (1988).
5. Yu.M. Andreev, I.L. Vasin, P.P. Geiko, S.I. Dolgii, V.V. Zuev, O.Ya. Zyryanov, O.A. Romanovskii, S.V. Smirnov, and S.F. Shubin, in: *Results of "Vertical-86" and "Vertical-87" Complex Experiments* (Tomsk Scientific Center SB RAS, Toms, 1989), 103 pp.
6. Yu.M. Andreev, V.G. Voevodin, P.P. Geiko, V.A. Gorobets, O.G. Lanskaya, V.O. Petukhov, N.P. Soldatkin, and A.A. Tikhomirov, *Lidar Systems and their Optical-Electronic Elements* (IAO SB RAS, Tomsk, 2004), 525 pp.
7. T.-J. Wang, J.-Y. Gao, Q.-Y. He, T. Ma, Y. Jiang, and Z.-H. Kang, J. Appl. Phys. **98**, P073102 (2005).

8. Yu.M. Andreev, V.V. Badikov, V.G. Voevodin, L.G. Geiko, P.P. Geiko, M.V. Ivashchenko, A.I. Karapuzikov, and I.V. Sherstov, Quant. Electron. **31**, No. 12, 1075−1078 (2001).

9. N.P. Barnes, R.C. Eckhard, D.J. Gettemy, and L.B. Edgett, IEEE J. Quantum Electron. **QE-15**, No. 10, 1074−1076 (1979).

10. V.G. Dmitriev, G.G. Gurzadyan, and D.N. Nikogosyan, *Handbook of Nonlinear Optical Crystals* (Springer-Verlag, 1999), 413 pp.

11. E. Takaoka and K. Kato, in: OSA Tech. Digest. CLEO '98. (Washington. DC, 1998), pp. CFH7. P. 253−254.

12. P. Schunemann, Laser Focus World, No. 4, 85−90 (1999).

13. Yu.M. Andreev, P.P. Geiko, and M.V. Kabanov, Avtometriya **40**, No. 5, 119−133 (2004).

14. K.R. Allakhverdiev, R.I. Guliev, E.Yu. Salaev, and V.V. Smirnov, Sov. J. Quant. Electr. **12**, No. 7, 947−948 (1982).

15. L.K. Samanta, D.K. Ghosh, amd G.C. Bhar, Phys. Rew. **35**, No. 9, 4519−4521 (1987).

16. T.-J. Wang, Q.-Y. He, Z.-H. Kang, H.-Z. Zhang, Y. Jiang, Z.-S. Feng, J.-Y. Gao, Yu. Andreev, G. Lanskii, V. Atuchin, and O. Parasyuk, Appl. Phys. Lett. **90**, P181913 (2007).

17. Y. Qu, Z.-H. Kang, T.-J. Wang, Y. Jiang, Y.M. Andreev, and J.-Y. Gao, Laser Phys. Lett. **4**, No. 3, 238−241 (2006).